Microchimica Acta
https://doi.org/10.1007/s00604-018-3056-3

ORIGINAL PAPER

Aerogels prepared from polymeric β-cyclodextrin and graphene aerogels as a novel host-guest system for immobilization of antibodies: a voltammetric immunosensor for the tumor marker CA 15–3

Haiyan Jia[1,2] · Qingyun Tian[1] · Jingkun Xu[1,3] · Limin Lu[2] · Xue Ma[2] · Yongfang Yu[2]

Received: 10 July 2018 / Accepted: 18 October 2018

Abstract

A three-dimensional porous network graphene aerogel (GAs) with large specific area and excellent conductivity was loaded with β-cyclodextrin polymer (Pβ-CD) to serve as a support for immobilization of antibodies. A highly sensitive immunosensor for the cancer marker carbohydrate antigen 15–3 (CA15–3) was designed based on the use of Pβ-CD/GAs. The large specific area of GAs warrants high loading with antibodies, and their excellent electrical conductivity warrants strong electrical signals. Based on the synergistic effect of GAs and Pβ-CD, an immunoassay was designed that is making use of hexacyanoferrate as an electrochemical probe and having a pleasantly low working potential of 0.2 V (vs. SCE). Response is linear in the 0.1 mU mL^{-1} to 100 U mL^{-1} activity range, and the lower detection limit is 0.03 mU mL^{-1} (at $S/N = 3$). The immunoassay is stable, selective and reproducible. It was applied to the analysis of spiked samples, and results were satisfactory.

Keywords β-Cyclodextrin polymer · Three-dimensional structure · Biosensor · Carbohydrate antigen 15–3 · Immunoassay · Host-guest immobilization · Breast cancer · Human serum · Biomarker

Introduction

Breast cancer (BC) is one of the malignant tumors that threaten the health of women of all ages. Moreover, the mortality rate of BC is constantly increasing [1–3]. As the main specific biomarker of BC, the level of carbohydrate antigen 15–3 (CA15–3) in blood serums can provide some information for early diagnosis and therapy of BC [4, 5]. Therefore, rapid and accurate detection of CA15–3 concentration is critical [6, 7]. Electrochemical immunoassay has attracted great attention in detecting tumor marker because of its fast response, high sensitivity and selectivity [8–11]. However, in the serums of early cancer patients, the level of tumor marker is extremely low, which results in a great challenge in monitoring. Hence, improving the sensitivity of immunoassay for detecting tumor marker has become the current focus of scientific research.

Electrode interface and antibody immobilized method are two of the most important factors influencing the sensitivity of the immunosensor [12–15]. Usually, noble metal nanoparticles including Au nanoparticles (Au NPs), Pt nanoparticles (Pt NPs) and Pd nanoparticles (Pd NPs) are applied to immobilize antibody via adsorption due to their high surface free energy [16]. The method is effective, but these noble nanoparticles are expensive. In addition, crosslinking and covalent bonding are two of the most common cheap methods for antibody immobilization. However, the procedures involved in the

Electronic supplementary material The online version of this article (https://doi.org/10.1007/s00604-018-3056-3) contains supplementary material, which is available to authorized users.

✉ Jingkun Xu
xujingkun1971@yeah.net; xujingkun@tsinghua.org.cn

✉ Limin Lu
lulimin816@hotmail.com

[1] School of Pharmacy, Jiangxi Science and Technology Normal University, Nanchang 330013, People's Republic of China

[2] Institute of functional materials and agricultural applied chemistry, College of Science, Jiangxi Agricultural University, Nanchang 330045, People's Republic of China

[3] School of Chemistry and Molecular Engineering, Qingdao University Science and Technology, Qingdao 266042, People's Republic of China

Published online: 25 October 2018

two methods are cumbersome and time-consuming, and the use of cross-linking agents, such as glutaraldehyde can reduce the activity of antibody [17, 18]. Therefore, developing a low-cost and green antibody fixation method is essential in fabricating high-performance immunosensor.

β-Cyclodextrin (β-CD), a toroidal shape oligosaccharide, possesses a hydrophobic inner cavity and a hydrophilic exterior. The hydrophobic inner cavity of β-CD can selectively bind various organic, inorganic, and biological guest molecules into its cavities to form host-guest inclusion complexes [19–22]. The antibody with amino functional groups can bind in the inner cavity of β-CD through the host-guest interaction. This unique feature has been promoted as novel immobilization method for antibody in immunoassay. Unfortunately, owing to the good water-solubility of β-CD, the stability of the immunosensor is poor [23]. In contrast, the β-cyclodextrin polymer (Pβ-CD) shows higher stability than β-CD. Pβ-CD can also provide a number of β-CD units to bind the guest molecules [24]. However, the Pβ-CD displays poor conductivity and dispersity. To solve these problems, some conductive materials were introduced into Pβ-CD. For example, Chen et al. [25] fabricated a prion immunosensor based on Pβ-CD/Au NPs composite platform. Au NPs with excellent conductivity as the bridge between Pβ-CD and glass carbon electrode (GCE) not only enhanced the electron transfer at the electrode interface, but also facilitated the immobilization of antibodies. As a result, the immunosensor exhibited high sensitivity. Li et al. [26] prepared a nonenzymatic electrochemical sensor for uric acid based on Pβ-CD/carbon nanotube ionic-liquid. The synergistic effect between Pβ-CD and carbon nanotube ionic-liquid obviously enhanced the detection sensitivity of the sensor for uric acid.

Three-dimensional (3D) graphene aerogels (GAs) self-assembled with two-dimensional (2D) graphene sheets possess excellent electrical conductivity, good chemical and environmental stability and larger specific area [27, 28]. GAs as carriers of functional materials enlarge the specific surface area and enhance the conductivity of the material, and thus improve the electrocatalytic properties of composite materials. For instance, Chen et al. [29] reported the preparation of 3D porous redox-active prussian blue/graphene aerogels (PB/GAs) and the composite modified electrode was employed as electrochemical H_2O_2 sensor. The 3D PB/GAs owns large accessible surface area, high conductivity, and the joint effect of PB and GAs, which enables excellent detection performance for H_2O_2. Our group [30] reported an enzyme-free electrochemical sensor for organophosphate pesticide malathion detection based on CuO-NPs/GAs. The interconnected microporous GAs provided large specific area for the loading of CuO nanoparticles, which offered a large number of active sites for malathion adsorption and enhanced sensing performance. Based on these excellent properties of GAs, it is believed that GAs can be employed as an ideal carrier to load Pβ-CD. However, to the best of our knowledge, the composite of Pβ-CD and GAs as the immunosensing platform has not been reported.

Herein, 3D GAs were synthesized by a hydrothermal method and the β-CD was polymerized on the surface of GAs by electropolymerization method. Then a novel label-free immunosensor for detecting CA 15–3 was designed using Pβ-CD/GAs nanocomposite as the sensing matrix, in which anti-CA 15–3 was fixed on the sensing interface via host-guest interaction between Pβ-CD and antibody. The designed immunosensor presented high sensitivity because of the advantages of Pβ-CD/GAs nanocomposite, including large specific area, good biocompatibility and high supramolecular recognition ability.

Experimental

Reagents and material

Graphene oxide (GO) with the lateral size of 0.5–5 μm and the thickness of 0.8–1.2 nm was received from XF NANO, INC (www.xfnano.com). Carbohydrate antigen 15–3 (CA 15–3) and anti-CA 15–3 were bought from Bosai Biotechnology Co., Ltd. (www.chinabiocell.com). Human serum was supplied by Jiangsu Baolai Biotechnology Co., Ltd. (www.jsmlsw.com). Bovine serum albumin (BSA) was obtained from Sigma-Aldrich (www.sigmaaldrich.com). β-Cyclodextrin (β-CD) and $HClO_4$ were purchased from Aladdin Chemistry Co., Ltd. (www.aladdin-e.com). Phosphate buffered (PB) solution (0.1 M) of different pH was obtained by mixing standard stock solutions of NaH_2PO_4 (0.1 M) and Na_2HPO_4 (0.1 M). Distilled water was used in the whole experimental process. All other reagents were of analytical grade.

Apparatus

The electrochemical measurements, including cyclic voltammetry (CV) measurement, different pulse voltammetry (DPV) measurement and electrochemical impedance spectroscopy (EIS) measurement, were performed on an electrochemical workstation (CHI 660D, Shanghai, China). The morphologies of various nanomaterials were taken with Hitachi S-4800 scanning electron microscopy (SEM, Hitachi, Japan). FT-IR spectrums of different materials were collected by Spectrum Two FT-IR Spectrometer (PerkinElmer, US). All electrochemical experiments were performed using a conventional three-electrode system containing a glass carbon electrode (GCE, $\varphi = 3$ mm) as the working electrode, a platinum sheet (counter electrode) and saturated calomel electrode (SCE, reference electrode). All potential values were cited versus SCE.

Preparation of GAs

The graphene hydrogel (GH) was prepared according to the reported literature with a little modification [31]. The experiment method is given in the Electronic Supporting Material. The surface water of GH was removed by freeze-drying at −60 °C for 24 h to obtain GAs.

A 0.1 mg mL^{-1} GAs suspension was prepared by dispersing 0.5 mg of GAs into 5 mL deionized water. The GAs suspension was sonicated for 30 min to obtain homogeneous dispersion. Reduced graphene oxide (rGO) was obtained by reducing GO with hydrazine hydrate using the Wallace method [32].

Preparation of the immunosensor

Prior to fabrication of immunosensor, the GCE was polished with 0.05 μm alumina powders and ultrasonically cleaned with distilled water, ethanol and distilled water, respectively. The GAs modified electrode (GAs/GCE) was obtained by casting the GAs dispersion (6 μL, 0.1 mg mL^{-1}) on the cleaned electrode surface and drying in air. The GAs/GCE was then immersed in the electrolyte solution (4 mL) containing 0.04 M β-CD and 1 M $HClO_4$, and the β-CD was electrochemical polymerized on GAs/GCE by CV in a potential range from 0 to 1.5 V with a scan rate of 100 mV s^{-1} [25]. After polymerization, the Pβ-CD/GAs/GCE was cleaned with distilled water to remove the electrolyte solution adsorbed on the electrode and dried in air.

To obtain the anti-CA 15–3/Pβ-CD/GAs/GCE, the Pβ-CD/GAs/GCE was incubated with anti-CA 15–3 (6 μL, 13.2 μg mL^{-1}) at 37 °C for 1.5 h, followed by washing with distilled water. To block the non-specific sites, BSA (6 μL, 0.1 wt%) was incubated on anti-CA 15–3/Pβ-CD/GAs/GCE for 15 min, and then washed with distilled water. The immunosensor (BSA/anti-CA15–3/Pβ-CD/GAs/GCE) was stored at 4 °C before use. The fabrication and detection process of the immunosensor is shown in Scheme 1.

Electrochemical measurements

The proposed immunosensor (BSA/anti-CA15–3/Pβ-CD/GAs/GCE) was incubated with various concentration of CA 15–3 (6 μL) for 1.5 h at 37 °C, followed by washing thorough with distilled water. The electrochemical immunoassay was conducted in PB solution (0.1 M, pH 7.0) with 5 mM $[Fe(CN)_6]^{3-/4-}$ and 0.1 M KCl. The evaluation of analytical performance of the immunosensor depends on the inhibition ratio ($\Delta I/I_0$), where, $\Delta I = (I_0\text{-}I)$, I and I_0 are the peak currents with and without antigen, respectively. Differential pulse voltammetry (DPV) measurement was performed from −0.2 to 0.6 V (vs. SCE) with pulse period of 0.2 s and amplitude of 50 mV. Electrochemical impedance spectroscopy (EIS) measurement was performed in the 0.1 Hz to 100 kHz frequency range with amplitude of 5 mV and the applied potential of 0.24 V.

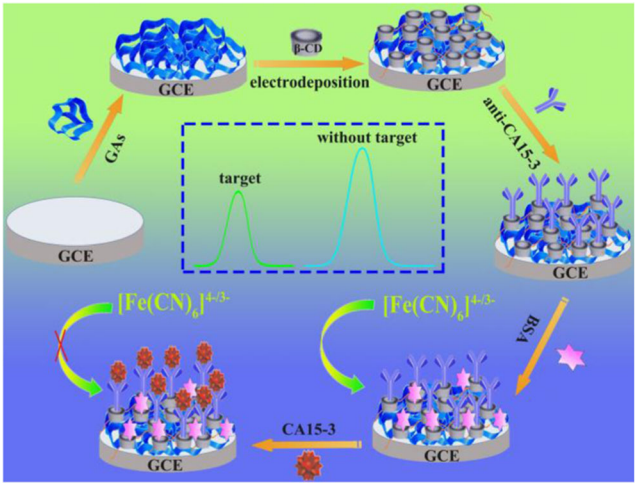

Scheme 1 The fabrication sequence of Pβ-CD/GAs based immunosensor for the detection of CA15–3

Results and discussion

Choice of materials

β-CD is well known for selectively binding various organic, inorganic and biological guest molecules, such as antibody due to its unique molecular structure containing a hydrophobic inner cavity and a hydrophilic exterior [33, 34]. β-cyclodextrin polymer (Pβ-CD) consisting of lots of β-CD units not only owns the unique properties of β-CD, but also shows higher stability as electrode material. These interesting characteristics enable Pβ-CD to be applied in the fabrication of electrochemical immunosensor [25]. Unfortunately, Pβ-CD shows poor conductivity. It can be rationalized that the utilization of carbon materials like graphene as the supporting materials might effectively circumvent the drawbacks of Pβ-CD [35, 36]. However, graphene is prone to agglomerate because of the strong π-π stacking of individual graphene. In contrast, 3D GAs with network structure can inhibit the restacking of individual graphene sheets. It not only possesses the intrinsic excellent properties of graphene, but also owns its unique adjustable pore structure, large specific surface area, good chemical and mechanical stability [27]. As a consequence, it can be expected that the combination of GAs with Pβ-CD serve as a high-performance immunosensing platform.

Characterization of different nanomaterials

Scanning electron microscopy (SEM) was applied to characterize the morphologies of different nanomaterials including

Pβ-CD (Fig. S1A), GAs (Fig. S1B) and Pβ-CD/GAs (Fig. S1C). The FT-IR spectrums were used to confirm the formation of Pβ-CD/GAs (Fig. S1D). These results indicated that the fabrication of Pβ-CD/GAs was successful. The detailed information was given in Electronic Supporting Material.

Electrochemical characterization of the immunosensor

The stepwise-modified process of the immunosensor was probed by differential pulse voltammetry (DPV). As shown in Fig. S2A, compared with bare GCE (curve a), higher peak current occurred at Pβ-CD/GAs modified GCE (curve b), which was due to the good conductivity of Pβ-CD/GAs nanocomposite. The peak current decreased when anti-CA 15–3 was incubated on Pβ-CD/GAs/GCE (curve c), since the nonconductive protein retarded the electron transfer toward the electrode surface. A further decrease of the peak current occurred when the remaining nonspecific sites were blocked by BSA (curve d). Finally, after modification in CA 15–3 (curve e), the current decreased owing to the formation of anti-CA15–3 and CA15–3 immunocomplexes impeded the electron conduction. All these results indicated that the construction of immunosensor was successful.

Electrochemical impedance spectroscopy (EIS) was further applied to characterize the fabrication process of the immunosensor. In Nyquist plot, the semicircle diameter at high frequencies is equal to the electron-transfer resistance (Ret). The linear portion at low frequencies responds to the diffusion step of the overall process [9]. As shown in Fig. S2B, bare GCE (curve a) showed a small semicircle, while the Ret significantly decreased after GCE was modified with Pβ-CD/GAs (curve b), which was because of the excellent conductivity of the nanocomposite. When anti-CA 15–3 was modified on Pβ-CD/GAs/GCE (curve c), an obvious increase in Ret was observed because the formation of blocking layer impeded the electron transfer. The Ret continued to increase upon the immobilization of BSA (curve d) and CA 15–3 (curve e) successively due to a barrier formed by proteins hindering the electron conductivity. These results illustrated that the immunosensor was successfully fabricated, which was consistent with that of the above measurement by DPV.

In order to understand the electrochemical mechanism, the cyclic voltammetry (CV) of the immunosensor at various scan rate (10–300 mV s^{-1}) was investigated. As shown in Fig. S3A, the redox peak current enhanced with the enlargement of scan rate. As indicated from Fig. S3B, the redox peak current was proportional to the square root of scan rate with the linear relationships as I_{pc} (cathodic peak current, μA) = 7.876x + 11.509 (R^2 = 0.9983) and I_{pa} (anodic peak current, μA) = −7.854x-9.910 (R^2 = 0.9993), indicating that the electrode reaction was a diffusion-controlled process.

The electrochemical surface area of the modified electrode can be calculated from the voltammetric peak current by use of the Randle-Sevcik equation [37]:

$$I_{pc} = 2.69 \times 10^5\ AD^{1/2}n^{3/2}v^{1/2}\ C$$

Where, I_{pc} is the cathodic peak current. A is the surface area. n is the number of electron involved in redox reaction (n = 1). D is the diffusion coefficient of the molecule in solution (7.6×10^{-6} cm^2 s^{-1}) [38]. C is the concentration of the probe molecule (5 mM $[Fe(CN)_6]^{3-/4-}$). v is the scan rate. From the slope of the I_{pc} - $v^{1/2}$ relationship (Fig. S3B), the electrochemical surface area for the electrode modified with Pβ-CD/GAs was 0.2122 cm^2.

Signal amplification

As controls, the immunosensor based on different nanomaterials, including BSA/anti-CA15–3/GAs/GCE, BSA/anti-CA15–3/Pβ-CD/GCE, BSA/anti-CA15–3/ Pβ-CD/rGO/GCE and BSA/anti-CA15–3/Pβ-CD/GAs/GCE were applied to detect CA15–3 (37 U mL^{-1}). The judgement is based on the inhibition ratio of the immunosensor towards the detection of CA15–3. As expected, the immunosensor of BSA/anti-CA15–3/Pβ-CD/GAs/GCE exhibited the highest inhibition ratio (37.77%), while the inhibition ratios of the immunosensor of BSA/anti-CA15–3/GAs/GCE, BSA/anti-CA15–3/Pβ-CD/GCE and BSA/anti-CA15–3/Pβ-CD/rGO/GCE were 10.45%, 15.64% and 20.39%, respectively (Fig. 1). This phenomenon can be attributed to the fact that the 3D porous GAs matrix possessed larger specific area than that of rGO, which increased the load number of Pβ-CD molecules and enhanced the sensitivity of the immunosensor.

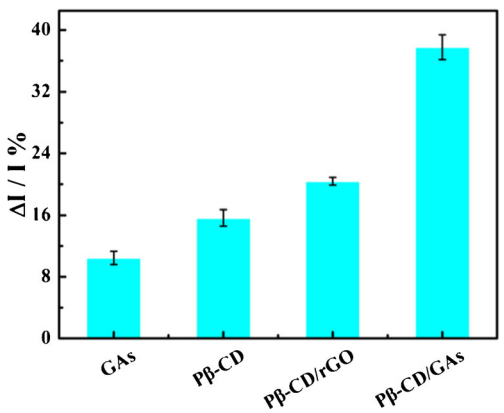

Fig. 1 Comparation of the detection performance for CA 15–3 (37 U mL^{-1}) using the immunosensor modified with different nanomaterials: GAs, Pβ-CD, Pβ-CD/rGO and Pβ-CD/GAs

Optimization of the method

The following parameters were optimized: (A) Electropolymerization cycles of β-CD; (B) concentration of GAs; (C) pH of detection solution; (D) incubation time of antibody; (E) incubation time of antigen; Respective data and Figures are given in the Electronic Supporting Material (Fig. S4). The following experimental conditions were found to give best results: (A) optimal electropolymerization cycle: 20; (B) best concentration of GAs: 0.1 mg mL^{-1}; (C) best pH of detection solution: pH 7.0; (D) optimal incubation time of antibody: 90 min; (E) optimal incubation time of antigen: 90 min.

Analytical performance of the assay

Based on the optimized experimental conditions, the immunosensor was applied to monitor various concentration of CA 15–3 by DPV. As expected, from Fig. 2a, we can clearly observe that the peak current reduced with the augment of the concentration of CA 15–3. As presented in Fig. 2b, the inhibition ratio and logarithm of the concentration of CA15–3 showed a good linear relationship from 0.1 mU mL^{-1} to 100 U mL^{-1}. The linear equation was $y = 2.607x + 35.97$ ($R^2 = 0.9993$) and the detection limit was estimated to be 0.03 mU mL^{-1} ($S/N = 3$). The sensitivity of the immunosensor was calculated to be 1.14 $\mu A \cdot (U\ mL^{-1})^{-1} \cdot cm^{-2}$. Moreover, the performance of the prepared immunosensor was compared with that of previously reported immunosensor. From Table S1, we can see that the immunosensor showed a lower detection limit than that of the previous reported [39–41]. The good analytical performance was mainly due to the following aspects: 1) GAs possess excellent conductivity and the 3D interconnected framework can allow multidimensional electron transport; 2) The large specific area of 3D GAs can load a number of Pβ-CD and the immobilized Pβ-CD can effectively capture anti-CA 15–3 to form stable host-guest complex.

Selectivity, reproducibility and stability

To verify the selectivity of the immunosensor, 100 ng mL^{-1} of interferents, including prostate specific antigen (PSA), bovine serum albumin (BSA), glucose (Glu), α-fetoprotein (AFP), ascorbic acid (AA), with and without 1 U mL^{-1} of CA 15–3 solution were measured using the immunosensor. As shown in Fig. 3, the variation of inhibition ratio was less than 5% of that without interferents, indicating that the immunosensor possessed an acceptable selectivity.

The reproducibility of the immunosensor was investigated using five identical fabricated immunosensor for detecting CA 15–3 (1 U mL^{-1}). The relative standard deviation (RSD) of the tests for five immunosensor was 2.67%, suggesting satisfactory reproducibility of the immunosensor.

To assess the long-term stability of the immunosensor, the fabricated immunosensor was stored in refrigerator at 4 °C and measured at an interval of every 2 days. After storage for 2 weeks, the current retained 95.17% of the original current measured. The result confirmed the immunosensor had good stability.

Reversibility

The reversibility of the immunosensor was investigated by detecting 100 U mL^{-1} CA 15–3 with the same immunosensor. After detecting CA 15–3, the electrode was immersed in a base solution containing 0.2 M NaOH and 0.5 M NaCl for 30 min to disrupt the antibody-antigen bonds and then washed with distilled water. The consecutive measurements were repeated five

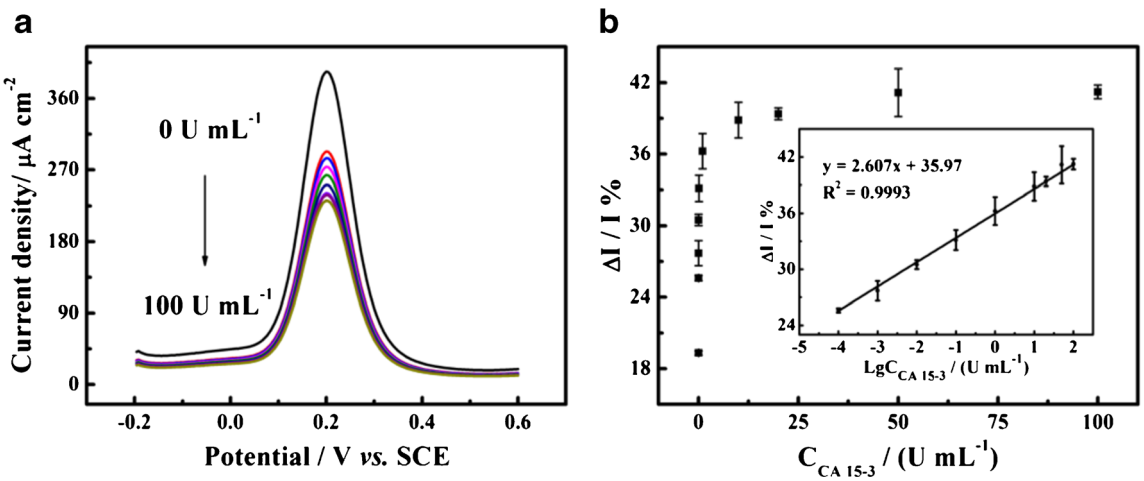

Fig. 2 **a** DPV responses of the immunosensor after immobilization with different concentrations of CA15–3 (0, 0.0001, 0.001, 0.01, 0.1, 1, 10, 20, 50 and 100 U mL^{-1}). **b** Calibration plot for CA 15–3 determination at the working potential of 0.2 V (vs. SCE) in 0.1 M PB solution (pH = 7.0) containing 5 mM $[Fe(CN)_6]^{3-/4-}$ and 0.1 M KCl. Inset: Linear plot of the immunosensor inhibition ratio vs logarithmic concentration of CA15–3. Error bar = SD ($n = 3$)

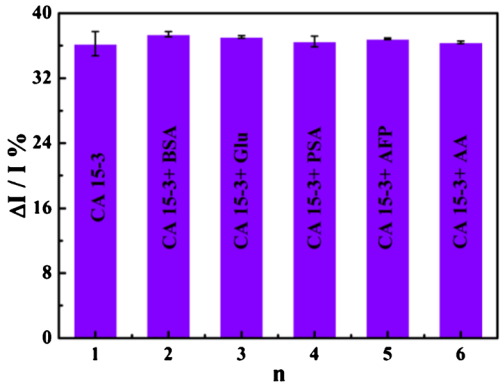

Fig. 3 Inhibition ratio of the immunosensor to (1) 2 U mL^{-1} CA15–3; (2) 2 U mL^{-1} CA15–3 + 100 ng mL^{-1} BSA; (3) 2 U mL^{-1} CA15–3 + 100 ng mL^{-1} glucose; (4) 2 U mL^{-1} CA15–3 + 100 ng mL^{-1} PSA; (5) 2 U mL^{-1} CA15–3 + 100 ng mL^{-1} AFP and (6) 2 U mL^{-1} CA15–3 + 100 ng mL^{-1} ascorbic acid. Error bar = SD ($n = 3$)

times, and the RSD was 4.7%. These results indicated that the reversibility of the immunosensor was acceptable.

Real sample analysis

The immunoassay of CA 15–3 in human serum sample was carried out using recovery test by spiking different known amounts of CA15–3 into serum samples to test the accuracy of the electrochemical quantification approach. The human serum sample obtained from Bosai Biotechnology Co., Ltd. was diluted one hundred times with PB solution (0.1 M, pH = 7.0) and mixed with different concentrations of CA 15–3 (0, 0.001, 0.1, 1, 20 U mL^{-1}). The samples were detected by DPV method and the response of current was recorded at 0.2 V (vs. SCE) with hexacyanoferrate as the redox probe. The recoveries were found to be between 99.43%–103.57% with the RSD ($n = 3$) less than 3.59% (Table S1). These results manifested that the immunosensor can be applicable for serum sample analysis.

In order to further evaluate the feasibility of the immunosensor for clinical application, three serum samples obtained from the Jiangxi Tumor Hospital (Nanchang, China) was measured. The result was compared with the commercial enzyme-linked immunosorbent assay (ELISA) method. As shown in Table S3, the results from our proposed method were in good agreement with ELISA method. And the relative error between the two methods was in the range from −5.3%-3.47%, suggesting the feasibility of the immunosensor for the clinical determination of CA 15–3.

Conclusions

In summary, a sensitive label-free electrochemical immunosensor was successfully constructed and realized the quantitative detection of CA15–3 using 3D Pβ-CD/GAs composite as the efficient platform. The antibody immobilization principle is based on the host-guest interaction between β-CD and antibody. GAs was employed as support for high dispersion of Pβ-CD. Besides, the excellent conductivity of GAs accelerates the electron transfer between the mediator of hexacyanoferrate and the electrode, which resulted in an amplified electrochemical detection signal. The proposed label-free electrochemical immunosensor possessed excellent specificity, good reproducibility and acceptable stability. Therefore, this designed strategy might provide an effective candidate in clinical research.

Acknowledgements We are grateful to the National Natural Science Foundation of China (21665010, 31741103, 51572117 and 51302117), the outstanding youth fund and 5511 Project of Jiangxi Province (20162BCB23027 and 20165BCB18016), Jiangxi Provincial, Department of Education (GJJ12595), Natural Science Foundation of Jiangxi Province (20171BAB203015) for their financial support of this work.

Compliance with ethical standards The author(s) declare that they have no competing interests.

References

1. Darwish IA, Wani TA, Khalil NY, Blake DA (2012) Novel automated flow-based immunosensor for real-time measurement of the breast cancer biomarker CA15-3 in serum. Talanta 97:499–504
2. Khoshroo A, Mazloum-Ardakani M, Forat-Yazdi M (2018) Enhanced performance of label-free electrochemical immunosensor for carbohydrate antigen 15-3 based on catalytic activity of cobalt sulfide/graphene nanocomposite. Sensors Actuators B Chem 255:580–587
3. Zhao Y, Zheng YQ, Zhao CY, You JM, Qu FL (2015) Hollow PDA-Au nanoparticles-enabled signal amplification for sensitive nonenzymatic colorimetric immunodetection of carbohydrate antigen 125. Biosens Bioelectron 71:200–206
4. Jiang XY, Wang HQ, Yuan R, Chai YQ (2015) Sensitive electrochemiluminescence detection for CA15-3 based on immobilizing luminol on dendrimer functionalized ZnO nanorods. Biosens Bioelectron 63:33–38
5. Li YY, Xu CX, Li H, Wang H, Wu D, Ma HM, Cai YY, Du B, Wei Q (2014) Nonenzymatic immunosensor for detection of carbohydrate antigen 15-3 based on hierarchical nanoporous PtFe alloy. Biosens Bioelectron 56:295–299
6. Li H, He J, Li S, Turner AP (2013) Electrochemical immunosensor with N-doped graphene-modified electrode for label-free detection of the breast cancer biomarker CA 15–3. Biosens Bioelectron 43:25–29
7. Zhao LF, Wei Q, Wu H, Dou JK, Li H (2014) Ionic liquid functionalized graphene based immunosensor for sensitive detection of carbohydrate antigen 15-3 integrated with Cd^{2+}-functionalized nanoporous TiO_2 as labels. Biosens Bioelectron 59:75–80
8. Afsharan H, Khalilzadeh B, Tajalli H, Mollabashi M, Navaeipour F, Rashidi MR (2016) A sandwich type immunosensor for ultrasensitive electrochemical quantification of p53 protein based on gold nanoparticles/graphene oxide. Electrochim Acta 188:153–164
9. Mazloum-Ardakani M, Hosseinzadeh L, Khoshroo A (2015) Label-free electrochemical immunosensor for detection of tumor necrosis factor α based on fullerene-functionalized carbon nanotubes/ionic liquid. J Electroanal Chem 757:58–64
10. Pei HM, Zhu SY, Yang MH, Kong RM, Zheng YQ, Qu FL (2015) Graphene oxide quantum dots@ silver core-shell nanocrystals as

turn-on fluorescent nanoprobe for ultrasensitive detection of prostate specific antigen. Biosens Bioelectron 74:909–914
11. Zhao Y, Zheng YQ, Kong RM, Xia L, Qu FL (2016) Ultrasensitive electrochemical immunosensor based on horseradish peroxidase (HRP)-loaded silica-poly (acrylic acid) brushes for protein biomarker detection. Biosens Bioelectron 75:383–388
12. Wang J, Yang DC, Chen MF, Liu BF, Chen H, Xu H, Wang WX, Bai LJ (2018) Electrochemical Immunosensor detection of tumor markers based on GO composite Nanoprobe for signal amplification. Anal Methods 10:526–532
13. Chen Y, Li Y, Deng DM, He HB, Yan XX, Wang ZX, Fan CH, Luo LQ (2018) Effective immobilization of Au nanoparticles on TiO_2 loaded graphene for a novel sandwich-type immunosenso. Biosens Bioelectron 102:301–306
14. Li Y, He JL, Chen J, Niu YZ, Zhao YL, Zhang YC, Yu C (2018) A dual-type responsive electrochemical immunosensor for quantitative detection of PCSK9 based on n-C_{60}-PdPt/N-GNRs and Pt-poly (methylene blue) nanocomposites. Biosens Bioelectron 102:301–306
15. Han J, Zhang MF, Chen GJ, Zhang YQ, Wei Q, Zhuo Y, Xie G, Yuan R, Chen SQ (2017) Ferrocene covalently confined in porous MOF as signal tag for highly sensitive electrochemical immunoassay of amyloid-β. J Mater Chem B 5:8330–8336
16. Huang KJ, Niu DJ, Xie WZ, Wang W (2010) A disposable electrochemical immunosensor for carcinoembryonic antigen based on nano-Au/multi-walled carbon nanotubes-chitosans nanocomposite film modified glassy carbon electrode. Anal Chim Acta 659:102–108
17. Zhang XY, Shen GY, Sun SY, Shen YM, Zhang CX, Xiao AG (2014) Direct immobilization of antibodies on dialdehyde cellulose film for convenient construction of an electrochemical immunosensor. Sensors Actuators B Chem 200:304–309
18. Chen S, Zhang JB, Gan N, Hu FT, Li TH, Cao YT, Pan DD (2015) An on-site immunosensor for ractopamine based on a personal glucose meter and using magnetic β-cyclodextrin-coated nanoparticles for enrichment, and an invertase-labeled nanogold probe for signal amplification. Microchim Acta 182(3–4):815–822
19. Ortiz M, Fragoso A, O'Sullivan CK (2011) Amperometric detection of antibodies in serum: performance of self-assembled cyclodextrin/cellulose polymer interfaces as antigen carriers. Org Biomol Chem 9(13):4770–4773
20. Niu XH, Mo ZL, Yang X, Sun MY, Zhao P, Li ZL, Ouyang MX, Liu ZY, Gao HH, Guo RB, Liu NJ (2018) Advances in the use of functional composites of β-cyclodextrin in electrochemical sensors. Microchim Acta 185(7):328
21. Zhu GB, Yi YH, Chen JH (2016) Recent advances for cyclodextrin-based materials in electrochemical sensing. TrAC Trends Anal Chem 80:232–241
22. Gao YS, Wu LP, Zhang KX, Xu JK, Lu LM, Zhu XF, Wu Y (2015) Electroanalytical method for determination of shikonin based on the enhancement effect of cyclodextrin functionalized carbon nanotubes. Chin Chem Lett 26:613–618
23. Zhang Y, Yuan R, Chai YQ, Li WJ, Zhong X, Zhong HA (2011) Simultaneous voltammetric determination for DA, AA and NO_2^- based on graphene/poly-cyclodextrin/MWCNTs nanocomposite platform. Biosens Bioelectron 26:3977–3980
24. Zhang X, Wu L, Zhou JW, Zhang XH, Chen JH (2015) A new ratiometric electrochemical sensor for sensitive detection of bisphenol A based on poly-β-cyclodextrin/electroreduced graphene modified glassy carbon electrode. J Electroanal Chem 742:97–103
25. Li XY, Li JJ, Liu YQ, Zhang XH, Chen JH (2017) A sensitive electrochemical immunosensor for prion detection based on poly-β-cyclodextrin/gold nanoparticles/glassy carbon electrode. Sensors Actuators B Chem 250:1–7
26. Li YH, Zhai XR, Wang HB, Liu XS, Guo L, Ji XL, Wang L, Qiu HY, Liu XY (2015) Non-enzymatic sensing of uric acid using a carbon nanotube ionic-liquid paste electrode modified with poly(β-cyclodextrin). Microchim Acta 182:1877–1884
27. Liu X, Sun JB, Zhang XT (2015) Novel 3D graphene aerogel-ZnO composites as efficient detection for NO_2 at room temperature. Sensors Actuators B Chem 211:220–226
28. Xiao L, Wu DQ, Han S, Huang YS, Li S, He M, Zhang FZ, Feng XL (2013) Self-assembled Fe_2O_3/graphene aerogel with high lithium storage performance. ACS Appl Mater Interfaces 5:3764–3769
29. Chen L, Wang X, Zhang X, Zhang H (2012) 3D porous and redox-active prussian blue-in-graphene aerogels for highly efficient electrochemical detection of H_2O_2. J Mater Chem 22:22090–22096
30. Xie Y, Yu Y, Lu L, Ma X, Gong L, Huang X, Liu G, Yu Y (2018) CuO nanoparticles decorated 3D graphene nanocomposite as non-enzymatic electrochemical sensing platform for malathion detection. J Electroanal Chem 812:82–89
31. Xu YX, Sheng KX, Li C, Shi GQ (2010) Self-assembled graphene hydrogel via a one-step hydrothermal process. ACS Nano 4:4324–4330
32. Li D, Müller MB, Gilje S, Kaner RB, Wallace GG (2008) Processable aqueous dispersions of graphene nanosheets. Nature Nanotech 3:101–105
33. Zaidi SA (2017) Facile and efficient electrochemical enantiomer recognition of phenylalanine using β-Cyclodextrin immobilized on reduced graphene oxide. Biosens Bioelectron 94:714–718
34. Gao JJ, Liu MX, Song HO, Zhang SP, Qian YY, Li AM (2016) Highly-sensitive electrocatalytic determination for toxic phenols based on coupled cMWCNT/cyclodextrin edge-functionalized graphene composite. J Hazard Mater 318:99–108
35. Jiang ZM, Li GY, Zhang MX (2016) Electrochemical sensor based on electro-polymerization of β-cyclodextrin and reduced-graphene oxide on glassy carbon electrode for determination of gatifloxacin. Sensors Actuators B Chem 228:59–65
36. Qin Q, Bai X, Hua ZL (2016) Electropolymerization of a conductive β-cyclodextrin polymer on reduced graphene oxide modified screen-printed electrode for simultaneous determination of ascorbic acid, dopamine and uric acid. J Electroanal Chem 782:50–58
37. Bard AJ, Faulkner LR (2001) Electrochemical methods: fundamentals and applications, 2nd edn. Wiley, Hoboken
38. Zhou Y, Yang YJ, Deng X, Zhang GM, Zhang Y, Zhang CH, Shuang SM, He YJ, Sun W (2018) Electrochemical sensor for determination of ractopamine based on aptamer/octadecanethiol Janus particles. Sensors Actuators B Chem 276:204–210
39. Jiang LP, Han J, Li FY, Gao J, Li YY, Dong YH, Wei Q (2015) A sandwich-type electrochemical immunosensor based on multiple signal amplification for α-fetoprotein labeled by platinum hybrid multiwalled carbon nanotubes adhered copper oxide. Electrochim Acta 160:7–14
40. Nguyen V-A, Nguyen HL, Nguyen DT, Do QP, Tran LD (2017) Electrosynthesized poly(1,5-diaminonaphthalene)/polypyrrole nanowires bilayer as an immunosensor platform for breast cancer biomarker CA 15–3. Curr Appl Phys 17:1422–1429
41. Gomes RS, Moreira FT, Fernandes R, Sales MGF (2018) Sensing CA 15–3 in point-of-care by electropolymerizing O-phenylenediamine (oPDA) on Au-screen printed electrodes. PLoS ONE 13(5):e0196656